Active Sites for H_2 Adsorption and Activation in Au/TiO_2 and the Role of the Support†

Mercè Boronat,‡ Francesc Illas,§ and Avelino Corma*,‡

Instituto de Tecnología Química (UPV-CSIC), Av. de los Naranjos s/n, 46022 Valencia, Spain, and Departament de Química Física and Institut de Química Teòrica i Computacional (IQTCUB), Universitat de Barcelona, C/Martí i Franquès 1, E-08028 Barcelona, Spain

Received: September 17, 2008; Revised Manuscript Received: January 9, 2009

The catalytic activity toward H_2 dissociation of several Au nanoparticles of different shape, supported on stoichiometric and reduced TiO_2 surfaces, has been investigated by means of periodic DF calculations. Gold nanoparticles become positively charged when supported on stoichiometric TiO_2 and negatively charged when adsorbed on the reduced surface, although this finding does not appear to be relevant for H_2 dissociation activity. It is shown that Au atoms active for H_2 dissociation must be neutral or with a net charge close to zero, and be located at corner or edge low coordinated positions and not directly bonded to the support. The particles with the largest number of potentially active sites for H_2 dissociation are 2L isomers consisting of at least one bottom layer of gold atoms in contact with the support and therefore inactive, and one top layer with low coordinated gold atoms on which H_2 is adsorbed and activated. The presence of $O_{vacancy}$ defects in reduced surfaces preferentially stabilizes the most active 2L particles, while less active 1L isomers are the most stable on the stoichiometric surfaces.

1. Introduction

In contrast to chemically inert bulk gold,[1] small gold particles finely dispersed on inorganic oxide supports have attracted much attention in the last years as catalysts for a wide number of reactions including the water gas shift reaction,[2] CO and alcohol oxidation,[3−8] propylene epoxidation,[9,10] C−C bond formation,[11] and selective hydrogenations.[12−17] The activity of nanogold-based catalysts is usually related to structural effects such as the size and shape of the gold particles as well as to the nature of the interactions with the metal oxide support. It is also known that precise control of catalyst synthesis and activation procedures is a key factor to obtain active materials.[3]

The mechanism of CO oxidation and the effects responsible for the catalytic activity of gold nanoparticles toward this reaction have been experimentally[3−6,18,19] and theoretically[20−23] investigated. It seems to be generally accepted that the CO oxidation activity of gold nanoparticles is determined by the number of low coordinated gold atoms, which increases with decreasing particle size but is also dependent on particle shape.[24−26] There is also agreement concerning the higher oxidation activity of gold supported on reducible oxides such as TiO_2, Fe_2O_3, or CeO_2,[2−4,6,12] and although the mechanism of O_2 activation is unclear, it has been suggested that it occurs at the metal−support interface[27,28] or on oxygen vacancy defects present in reduced oxide surfaces.[29−31] With respect to the role of these oxygen vacancy defects, it has also been demonstrated that they act as nucleation sites for gold nanoparticles.[32]

In spite of its larger importance for industrial catalysis, selective hydrogenation on gold catalysts has received considerably less attention. It has been demonstrated experimentally that hydrogen is dissociated by gold atoms in corner or edge positions,[33] and it is suggested that besides the particle size, the shape of the gold particles plays a role on the catalyst activity for this process.[34] In this sense, the interaction with the support may induce particle shapes with varying amounts of low coordinated gold atoms, but it remains unknown whether the activity toward H_2 dissociation of sites at the metal−support interface is different from that of sites at the top of the particle. H_2 adsorption and dissociation on gold surfaces and on isolated gold particles of different size have been theoretically investigated,[35−42] and it has been shown that the active sites are low coordinated gold atoms, no matter whether they belong to defective extended surfaces or to large or small isolated particles. However, no theoretical study concerning the influence of the support on the H_2 dissociation activity of gold has been reported in the literature. We have now investigated the properties of different gold nanoparticles supported on TiO_2, focusing our attention on the relationship between gold particle shape, presence of oxygen vacancy defects in the support, and H_2 activation ability.

2. Model Catalysts and Computational Details

The interaction of molecular hydrogen on Au nanoparticles supported on TiO_2 was studied by means of periodic models by using large supercells to avoid interaction between the periodically repeated Au particles or between the repeated hydrogen molecules. For the TiO_2 support the anatase polymorph, most commonly used in experiments, and the corresponding (001) surface, the most reactive facet in anatase nanoparticles,[43,44] have been chosen and represented by a (4×4) supercell slab model. This model contains three TiO_2 layers and hence the unit cell contains 9 atomic layers and 144 atoms. A vacuum region larger than 20 Å was placed between vertically repeated slabs. This vacuum width is larger than the usual choices in the literature but one has to realize that since Au nanoparticles are later deposited on that support it is necessary to avoid any spurious interaction. Since it has been suggested that gold nanoparticles are initially formed on defects in the TiO_2 support[32] we considered, besides the stoichiometric surface,

† Part of the "George C. Schatz Festschrift".

* Corresponding author. E-mail: boronat@itq.upv.es, francesc.illas@ub.edu, acorma@itq.upv.es.

‡ Instituto de Tecnología Química (UPV-CSIC).

§ Universitat de Barcelona.

10.1021/jp808271y CCC: $40.75
Published on Web 02/10/2009

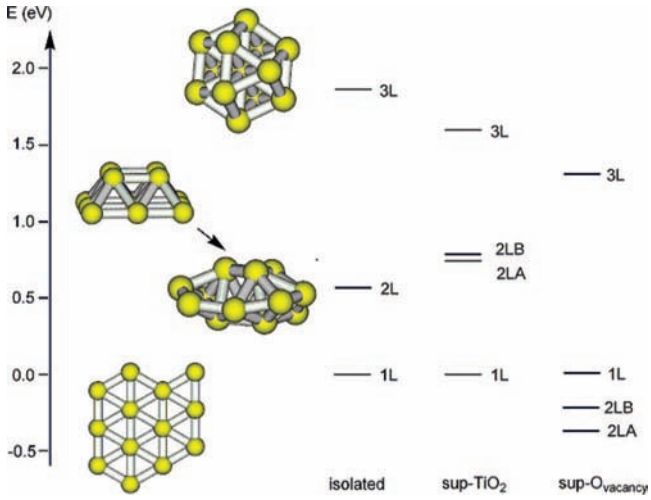

Figure 1. Relative stability of the different isomers of isolated and supported Au_{13} nanoparticles. The energy of the planar 1L particle has been taken as the origin of energies. The geometry of the isolated nanoparticles is depicted.

a surface with an O vacancy defect. The atomic positions of the two uppermost layers in the two models, regular and defective, were always fully relaxed and spin-polarization was included when necessary.

A nanoparticle containing 13 Au atoms, Au_{13}, has been chosen as representative of the ones used in the catalytic experiments for the chemoselective hydrogenation of nitroaromatic compounds.[16] Three different isomers of Au_{13} containing one (1L), two (2L), and three (3L) atomic layers have been considered which were directly cut out from bulk gold, placed in the same periodic box used to set up the supercell used for the TiO_2 support, and first optimized without the presence of the support. Particle 1L is planar and consists of 13 atoms belonging to the (111) surface (see Figure 1). Particle 2L initially consisted of two layers of 4 and 9 atoms parallel to the (001) surface and with (111) side facets. However, geometry optimization resulted in a particle with two atomic layers containing 10 and 3 atoms, respectively, and, not surprisingly, more or less parallel to (111), which is the most stable surface termination. Finally, particle 3L consists of three layers of 3, 7, and 3 atoms parallel to (111). In a second step, these Au_{13} particles were supported on the stoichiometric TiO_2 surface (sup-TiO_2) and on the surface model with one O vacancy point defect (sup-$O_{vacancy}$). For the supported particle models, the positions of all Au atoms and of the Ti and O atoms of the two uppermost atomic layers of the support were fully relaxed.

On the basis of the results of a previous computational study of the mechanism of H_2 dissociation on different gold catalyst models,[42] it has been assumed that only Au atoms able to bind molecular H_2 in a rather strong way will also be able to dissociate it. Consequently, the adsorption of molecular H_2 on different positions in the supported Au nanoparticles is the reactivity predictor parameter used to analyze the chemistry of these model catalysts. Thus, molecular H_2 was placed near different gold atoms in each of the supported nanoparticles, the position of the two H atoms, of all Au atoms, and of the Ti and O atoms of the two uppermost layers of the support were fully optimized, and the resulting geometries were analyzed and used to calculate adsorption energies.

Finally, and to better analyze and rationalize the results, the gold atoms in each nanoparticle were classified according to two different criteria: the coordination number (CN) or number of metal−metal bonds, and the geometrical arrangement (GA) of the neighboring atoms. The coordination number can be low (L) (2−3 metal−metal bonds), medium (M) (4−5 metal−metal bonds), or high (H) (6 or more metal−metal bonds). With respect to the geometrical arrangement we considered the following atom types: inside, terrace, edge, and corner. Inside atoms always have a large coordination number, terrace and edge atoms may have a high or medium coordination number, and corner atoms have a medium or low coordination number.

All calculations are based on density functional theory (DFT) and have been carried out with the VASP code,[45] using the perdew-Wang (PW91)[46] exchange-correlation functional within the Generalized Gradient Approximation (GGA). The Kohn−Sham orbitals used to obtain the electron density were expanded in a plane wave basis set with a kinetic energy cutoff of 415 eV, and the effect of the core electrons was taken into account by means of the Projected Augmented Wave (PAW) method.[47] Given the large size of the unit cell calculations were carried out at the Γ *k*-point of the Brillouin zone. The atomic positions were optimized by means of a conjugate-gradient algorithm until atomic forces were smaller than 0.01 eV/Å. Charge distributions were estimated by making use of the theory of atoms in molecules (AIM) of Bader.[48]

3. Results and Discussion

3.1. Structure and Relative Stability of Isolated Au_{13} Particles. The geometry and the relative stability of the three structural models of the isolated Au_{13} nanoparticle are depicted in Figure 1 whereas the description of the Au atoms in each structure is summarized in Table S1 in the Supporting Information. The most stable isomer is the planar 1L one. It has four atoms of terrace type, three of them with a coordination number equal to 6, three atoms in edge positions, and six atoms occupying corner sites. The spherical 3L particle is 1.82 eV less stable, and has one Au atom in the center surrounded by 12 corner Au atoms each with a coordination number of 5. For both 1L and 3L Au nanoparticles, the initial and optimized geometries are very similar. This is at variance of the situation found for the 2L nanoparticle, which upon optimization appears to be highly distorted from the structure cut from the bulk. This is not so surprising since the initial structure most exposed face is the less stable (001) one, while in the final optimized structure the particle consists of two layers of 10 and 3 atoms more or less parallel to (111). The geometrical arrangement of the atoms in the initial and optimized structures is quite similar, but the coordination number of all atoms has increased considerably.

3.2. Structure and Relative Stability of Supported Au_{13} Particles. The different Au_{13} isomers previously described and shown in Figure 1 were supported on the stoichiometric TiO_2 surface (sup-TiO_2) and on a O vacancy defect (sup-$O_{vacancy}$) model and their geometry was optimized as described above. Interaction with the support provokes noticeable deformations in the shape of the gold nanoparticles, especially in the case of the 2L and 3L isomers (see Figures 2 and 3), and important changes in their relative energies (see Figure 1). Since the results obtained for the two types of support considered are similar, they are described together in the following discussion. The optimized geometries of the supported nanoparticles together with the numbering of the gold atoms are depicted in Figures 2 and 3, and Table S2 in the Supporting Information summarizes the geometrical arrangement and bonding with the support of the gold atoms in each particle.

Adsorption of the 1L particle on the support does not modify the geometrical arrangement of the gold atoms, that is to say,

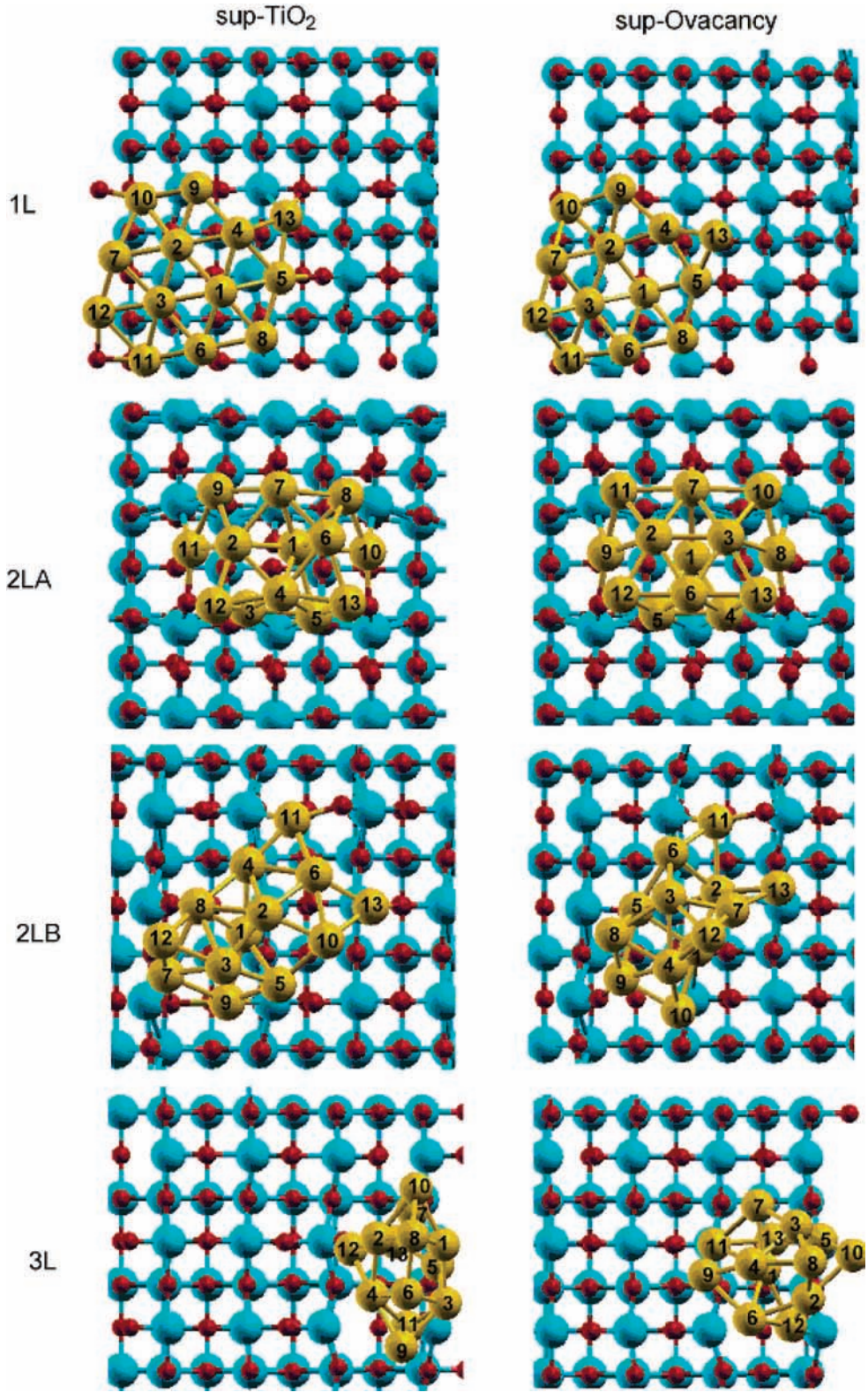

Figure 2. Top views of the different Au_{13} isomers supported on a stoichiometric (left) and a reduced (right) TiO_2 surface.

the number of terrace, edge, and corner atoms is conserved as in the isolated particle, but their coordination number increases due to the formation of Au−Ti bonds. As shown in Figure 3, particle 1L supported on stoichiometric TiO_2 maintains its planarity, but when it is deposited on a $O_{vacancy}$ defect, the terrace atom **1** is displaced downward to the center of the defect, while the edge atom **7** and especially the corner atoms **12** and **13** move upward, far from the oxide surface. For the 2L supported particles, two different cases were considered. Besides the fully optimized isolated particle, the initial structure directly cut out from the bulk was also adsorbed on the stoichiometric and reduced TiO_2 surfaces and optimized together with the support. In this last case, quite regular particles were obtained (2LA), with atom **1** inside the particle in contact with the support, and the rest of the Au atoms situated more or less symmetrically around it. This disposition causes a decrease in the number of

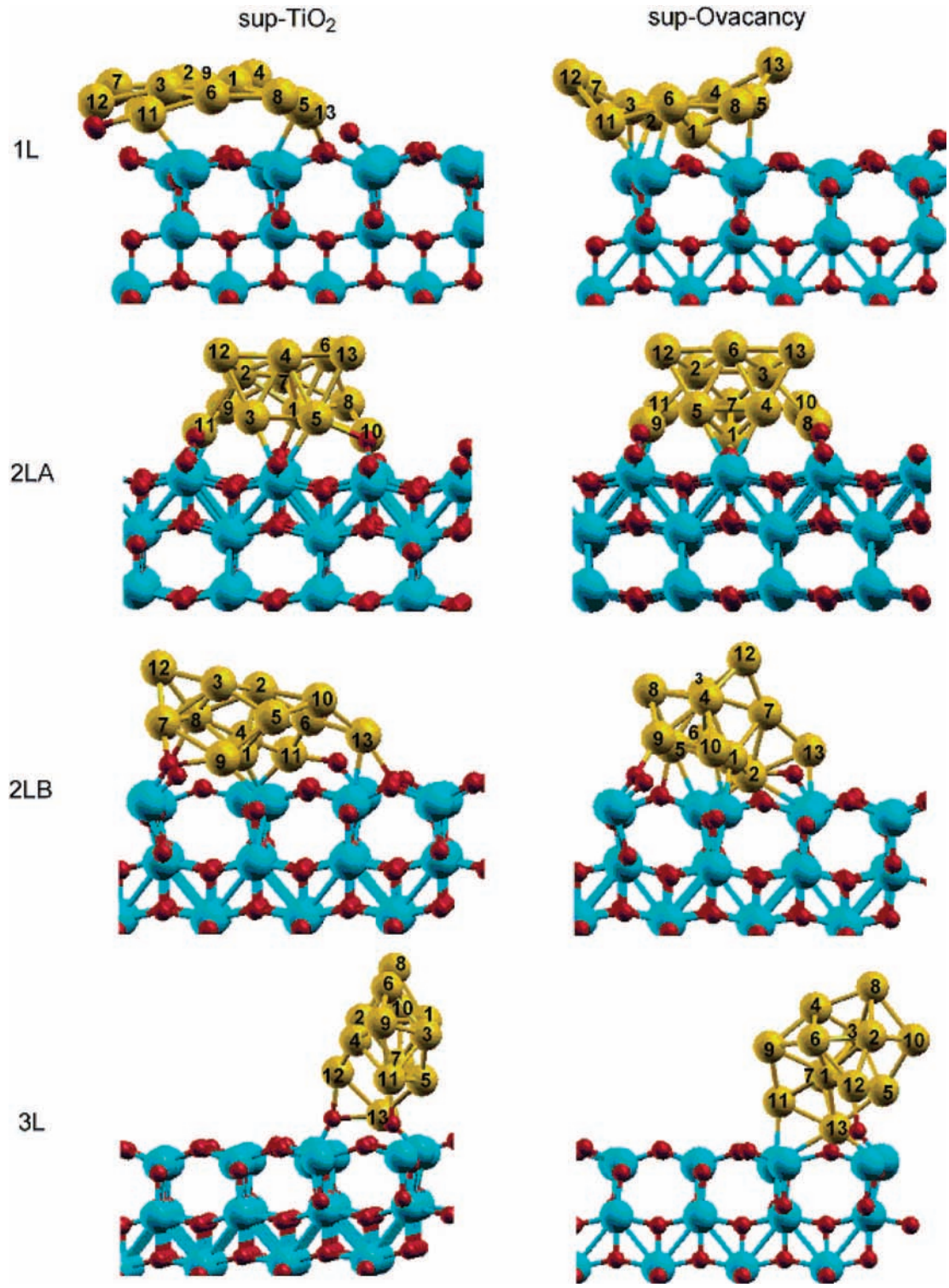

Figure 3. Side views of the different Au_{13} isomers supported on a stoichiometric (left) and a reduced (right) TiO_2 surface.

corner atoms with respect to the isolated particle, and an increase in the coordination number due to the formation of Au−Ti bonds (Table S2, Supporting Information). Adsorption of the fully optimized Au_{13} particle on TiO_2 results in highly distorted or irregular structures (2LB), with very different geometrical arrangements of the Au atoms. On stoichiometric TiO_2, the 2LB particle has only 3 corner atoms (**11**, **12**, and **13**), while the number of terrace and edge atoms has increased. On the $O_{vacancy}$ defect, two of the gold atoms, **1** and **2**, are inside the particle in contact with the support, but the number of corner atoms is still high. It should be noted that despite these geometrical differences, the regular 2LA isomer is only 0.03 eV on the TiO_2 support and 0.14 eV on the $O_{vacancy}$ defect more stable than the irregular 2LB system. This is a strong indication that the interaction with the support can indeed stabilize particle shapes which are very different from those of the isolated gas phase structures. This is clear from the results corresponding to the interaction of particle 3L with the support, which causes such a strong deformation that the particle practically looses its spherical shape and becomes a sort of distorted disk perpendicular to the oxide surface. Gold atoms in this system form few bonds with the atoms of the support, and tend to increase

TABLE 1: Adsorption, Deformation and Interaction Energies (in eV) and Net Charge on the Particle (in e) Calculated for Four Different Isomers of Au_{13} Nanoparticles Supported on Stoichiometric TiO_2 and on a $O_{vacancy}$ Defect

	sup-TiO_2				sup-$O_{vacancy}$			
	E_{ads}	E_{def}	E_{int}	q	E_{ads}	E_{def}	E_{int}	q
1L	−5.34	0.79	−6.13	+0.45	−4.53	1.07	−5.59	−0.46
2LA	−5.14	1.61	−6.74	+0.51	−5.41	1.40	−6.81	−0.05
2LB	−5.10	1.27	−6.38	+0.53	−5.27	1.27	−6.54	−0.20
3L	−5.55	−0.86	−4.69	+0.48	−5.04	−0.37	−4.66	−0.30

TABLE 2: Summary of Activity Data for H_2 Adsorption on the 1L Au_{13} Supported Particle

	atoms	CN	GA	O-bonded	adsorbs H_2?	E_{ads} (kcal/mol)	r_{HH} (Å)
1L sup-TiO_2	**5**	M	edge	yes	no	−0.65	0.75
	6−7	M	edge	no	yes	−3.91	0.82
	8−9	M	corner	no	yes	−4.89	0.81
	10−11	M	corner	yes	no[a]		
	12−13	L	corner	yes	no	−1.05	0.75
1L sup-$O_{vacancy}$	**5−6**	M	edge	no	no	−1.08	0.75
	7	M	edge	no	yes	−5.03	0.82
	8−9	M	corner	no	yes	−3.78	0.81
	10−11	M	corner	yes	no[a]		
	12−13	L	corner	yes	no	−5.13	0.81

[a] Equivalent to atoms **12−13** in particle 1L sup-TiO_2, directly bonded to O.

their coordination number through the formation of new Au−Au bonds. Thus, on the sup-TiO_2 system there is only one Au−Ti bond involving gold atom **13**, and when the 3L particle is adsorbed on the $O_{vacancy}$ defect only three atoms (**5**, **11**, and **13**) are directly bonded to Ti atoms of the oxide support. As a result of these geometrical arrangements, the number of corner atoms decreases considerably, and gold atoms in terrace and edge positions, which were lacking in the isolated particle, appear now. In the forthcoming discussion we will see that this has important implications for H_2 adsorption.

Analysis of Figure 1 reveals that the order of stability of the different Au_{13} isomers supported on stoichiometric TiO_2 follows that of the isolated nanoparticles, although the 2L structures have been destabilized and the 3L isomer has been stabilized with respect to the 1L particle, which is taken as reference. The situation on the $O_{vacancy}$ defective surface is slightly different; the less stable 3L isomer is only 1.3 eV higher in energy than the 1L (Figure 1) but the most stable species are now the 2L isomers. The scrutiny of the energetic data is completed by analysis of the adsorption energy (E_{ads}), deformation energy (E_{def},) and interaction energy (E_{int}) for each of the supported nanoparticles considered in this work, summarized in Table 1. The adsorption energy is calculated as the difference between the total energy of the Au_{13}-support system and the total energies of the support and the isolated particles separately:

$$E_{ads} = E(Au_{13}\text{-support})_{opt} - E(support)_{opt} - E(Au_{13})_{opt}$$

and therefore includes both the metal−support interaction and the effect of geometry relaxation of the gold nanoparticle. The definition of E_{def} and E_{int} allows us to decompose the interaction in meaningful contributions. The deformation energy is calculated as the difference between the energy of the Au_{13} nanoparticle in the conformation it adopts on the support and the energy of the corresponding isolated Au_{13} isomer:

$$E_{def} = E(Au_{13})_{supported\ geometry} - E(Au_{13})_{opt}$$

whereas the interaction energy has been calculated as the difference between the total energy of the Au_{13}-support system and the sum of the energies of the support and the particle in the conformation adopted on the support:

$$E_{int} = E(Au_{13}\text{-support})_{opt} - E(support)_{opt} - E(Au_{13})_{supported\ geometry}$$

TABLE 3: Summary of Activity Data for H_2 Adsorption on the 2L Au_{13} Supported Particle

	atoms	CN	GA	O-bonded	adsorbs H_2?	E_{ads} (kcal/mol)	r_{HH} (Å)
2LA sup-TiO_2	**6−9**	M	edge	no	yes	−3.95	0.82
	10−11	M	corner	no	no	−0.85	0.75
	12−13	L	corner	no	yes	−5.43	0.81
2LA sup-$O_{vacancy}$	**8−9**	M	corner	yes	no[a,b]		
	10−13	M	corner	no	yes	−9.77	0.81
2LB sup-TiO_2	**5−6**, **10**	M	edge	no	yes	−9.70	0.82
	7−8	M	edge	yes	no	−0.36	0.75
	9	M	edge	no	no[c]		
	12	L	corner	no	yes	−15.4	0.82
	11, **13**	L	corner	yes	no	−0.41	0.75
2LB sup-$O_{vacancy}$	**6−7**	M	edge	no	no	−0.49	0.75
	8	M	corner	no	yes	−6.76	0.83
	9	M	corner	yes	no	−1.33	0.75
	10	M	corner	no	yes	−3.40	0.79
	11	M	corner	yes	no	−0.85	0.75
	12−13	L	corner	no	yes	−3.15	0.80

[a] Equivalent to atoms **12−13** in particle 1L sup-TiO_2, directly bonded to O. [b] Equivalent to atoms **10−11** in particle 2LA sup-TiO_2, not easily accessible. [c] Nonaccessible.

Adsorption of gold nanoparticles on the TiO_2 support is energetically favorable in all cases, with calculated values for E_{ads} ranging between −4.5 and −5.5 eV. It is important to remark that no preferential stabilization on the $O_{vacancy}$ defects is found for similar gold nanoparticles although the presence of the $O_{vacancy}$ defects is probably necessary for nucleation to start. Nevertheless, adsorption energies on the stoichiometric and the reduced surfaces are similar for the 2L particles, while E_{ads} of the 1L particle on the $O_{vacancy}$ defect is 0.8 eV smaller than that on the stoichiometric surface, and the same trend is observed for the 3L particle. Deformation energies for the 1L and 2L particles are positive, meaning that there is an energy cost to change the particle shape from the gas phase to the adsorbed state that has to be compensated by the new bonds that are formed with the atoms of TiO_2 support. In the case of the 3L particle, however, the energy of the adsorbed on the support optimized structure is more stable than the almost spherical one cut out from the bulk, and therefore the specific metal−support interaction is the smallest. Thus, while the calculated E_{int} for the 3L particle is only −4.7 eV, the values obtained for the 2L isomers are almost −7 eV.

The analysis of the net charge on the Au atoms of the supported particle in Table S3 in the Supporting Information reveals that interaction of gold nanoparticles with the TiO_2 support involves a certain degree of charge transfer. The first clear-cut conclusion that can be obtained is that Au nanoparticles become slightly positively charged when adsorbed on stoichiometric TiO_2 and slightly negatively charged when the particles sit on top of an $O_{vacancy}$ defect. A second conclusion is that the net charge on the nanoparticle is not equally distributed among all atoms, but it is clearly localized on some of them. Thus, while most Au atoms remain neutral, with net charges between −0.05 and 0.05 e, some special atoms have net charges as large as +0.30 or −0.30 e. The gold atoms exhibiting a net positive charge larger than 0.1 e are always directly bonded to a O atom forming a Au−O−Ti bridge, with calculated O−Au distances between 2.0 and 2.3 Å. The O atoms directly bonded to Au

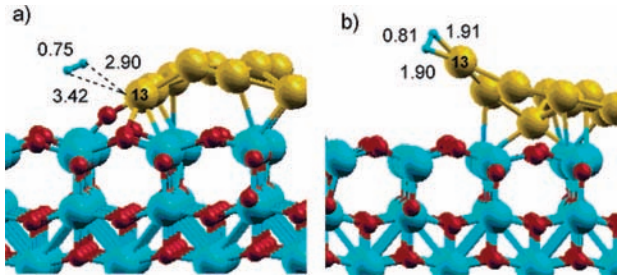

Figure 4. Optimized geometry of the structures corresponding to a nonadsorbed state of H_2 on a Au atom of particle 1L sup-TiO_2 (a) and to adsorbed H_2 on the same Au atom of particle 1L sup-$O_{vacancy}$.

atoms are less negatively charged (q_O between −0.93 and −0.99 e) than those coordinated only to Ti atoms (q_O between −1.01 and −1.16 e) while no special charging of Ti atoms directly coordinated to gold is observed. Negatively charged gold atoms are only found in particles supported on the $O_{vacancy}$ defect, and are usually inside or terrace-type atoms coordinated to six or more other Au or Ti atoms. Other Au atoms with a negative charge slightly larger than −0.1 e are low or medium coordinated gold atoms close to the oxide surface but not directly bonded to it.

3.3. Interaction of H_2 with the Supported Au_{13} Particles. The analysis of the structures of the supported Au_{13} in the previous subsection reveals the existence of a considerable number of nonequivalent Au atoms differing in coordination number, geometrical arrangement, net atomic charge, and neighboring atoms. To determine which are the characteristics of the most favorable sites for H_2 dissociation, it has been assumed that the mechanism necessarily involves the initial adsorption and activation of molecular H_2 on a low coordinated gold atom. Thus, only the initial adsorption step and not the global mechanism for each considered position, and only Au atoms with medium or low coordination number, and situated either in edge or corner positions, have been considered. This strategy permits one to disclose important trends while maintaining the computations feasible. Nevertheless, some highly coordinated positions have also been checked and it has been confirmed that they do not activate H_2. Also, special attention has been paid to Au atoms directly bonded to Ti or O, since their chemical reactivity might be different. The results obtained are summarized in Tables 24. Adsorption energies smaller than −1.5 kcal mol^{-1} are always associated to d_{HH} calculated bond length values of 0.75 Å, which is close to the optimized distance in the gas phase hydrogen molecule, and to Au−H optimized distances larger than 2.5 Å (not shown). Therefore, they clearly correspond to nonadsorbed (or weakly adsorbed) states (see Figure 4a). On the contrary, adsorption energies larger than −3.0 kcal mol^{-1} are related to structures such as that depicted in Figure 4b. The Au−H distances are 1.8−1.9 Å and the H−H bond lengths increase to more than 0.8 Å, indicating that molecular H_2 is activated and is therefore a probable precursor ready to dissociate.

As expected, and in agreement with previous results,[33,34,39,42] it has been found that most Au atoms in corner positions, either with low or medium coordination number, adsorb and activate H_2. Exceptions are, of course, those Au atoms that after adsorption on the support become inaccessible or are too close to the TiO_2 surface. The most interesting and unexpected result is, however, the finding that corner Au atoms with low coordination number and that are easily accessible by H_2 are not active sites for H_2 adsorption when they are directly bonded to an O atom. This is the case, for instance, for atoms **12** and **13** in particle 1L sup-TiO_2. As previously described, these atoms are involved in a Au−O−Ti bond and have a positive charge larger than 0.1 e. The optimized geometry of the H_2 adsorption complex on atom **13** depicted in Figure 4a shows an undistorted H_2 molecule at ∼3 Å from the Au atom. When the same 1L particle is supported on a $O_{vacancy}$ defect, Au atom **13** is not directly bonded to a O atom and is not positively charged, and in this case it does adsorb and activate H_2. As shown in Figure 4b and Tables 2−4, the H−H bond length increases to 0.81 Å, the Au−H distances are 1.90 Å, and the calculated adsorption energy is −5.13 kcal mol^{-1}. The same behavior is found for all corner and edge Au atoms belonging to a Au−O−Ti linkage: they do not activate H_2, no matter the particle shape or the nature of the support. With respect to edge atoms with medium coordination number and not directly bonded to O, they are also inactive when they belong to the bottom layer of the supported gold nanoparticle and are therefore close to the oxide surface. Altogether, it can be concluded that the active sites for H_2 dissociation in supported Au nanoparticles are corner or edge atoms in low coordination state, not directly bonded to O, and not belonging to the first atomic layer in contact with the support.

TABLE 4: Summary of Activity Data for H_2 Adsorption on the 3L Au_{13} Supported Particle

	atoms	CN	GA	O-bonded	adsorbs H_2?	E_{ads} (kcal/mol)	r_{HH} (Å)
3L sup-TiO_2	**6−7**	H	edge	no	no	−1.08	0.75
	8−10	M	corner	no	yes	−5.01	0.81
	11−12	M	corner	yes	no	−1.10	0.75
	13	M	corner	no	no[a]		
3L sup-$O_{vacancy}$	**6−7**	M	edge	no	yes	−9.06	0.84
	8	M	corner	no	yes	−3.28	0.80
	9−11	M	corner	no	no	−1.19	0.75
	12	L	corner	yes	no	−1.15	0.75
	13	H	corner	no	no[a]		

[a] Nonaccessible.

3.4. Implications for Catalyst Design. In this section we discuss how the results described can be used to tune the Au supported catalysts to maximize its activity toward H_2 dissociation. First, let us consider the one-layer particle. Although the 1L Au_{13} supported particles considered in this work contain 4−5 active atoms, this type of 1L particles do not seem to be the most interesting ones from a catalytic point of view, because the number of inactive terrace atoms will rapidly increase with increasing particle size, and because most of the remaining corner or edge atoms will always be in close contact with the support, which does not favor H_2 activation. On the other hand, only three of the thirteen atoms in the 3L particles have been found to be active for H_2 dissociation. This is in spite of the rather large number of accessible Au atoms and of the small number of direct bonds with the support in these systems. The reason is that most Au atoms in these particles, even those situated in edge positions, are directly bonded to a large number of other Au atoms, and therefore do not tend to increase their coordination number by interacting with H_2.

The analysis of the two-layer particles shows that three of the four 2L isomers studied in this work contain four Au atoms able to dissociate H_2. Since Au atoms directly bonded to O are unable to adsorb H_2 one could argue that the presence of $O_{vacancy}$ defects would increase the number of active sites, but this is not the case. Indeed, the largest number of Au active atoms is found in the most symmetrical 2LA nanoparticle supported on TiO_2. This system consists of one bottom layer of seven gold atoms in contact with the support and therefore inactive, and

one top layer of six low coordinated gold atoms separated from the support, and therefore active for H_2 dissociation. When the same particle is situated on the $O_{vacancy}$ defect, one gold atom moves downward inside the defect, and a large number of Au−Ti bonds are formed. As a result the particle shape changes and only four low coordinated Au atoms can be found on the top layer of the nanoparticle. However, slightly larger particles of this type will increase the number of low coordinated gold atoms on the top layer, becoming more similar to the 2LA sup-TiO_2 system. Finally, the beneficial effect of $O_{vacancy}$ defects is clearly seen when the relative stability of the different nanoparticles is taken into account. As shown in Figure 1, $O_{vacancy}$ defects preferentially stabilize two-layer particles, which are in general those having the largest number of active sites.

4. Conclusions

The catalytic activity toward H_2 dissociation of several Au nanoparticles of different shape supported on stoichiometric and reduced TiO_2 surfaces has been investigated by means of periodic DF calculations carried out by using realistic supercell models. Interaction with the support causes noticeable changes in the shape of the gold nanoparticles, and modifies their relative stability. 3L supported isomers are the least stable species, and the order of stability of 1L and 2L particles depends on the nature of the support: one-layer particles are the most stable on the stoichiomeric surfaces, while the presence of $O_{vacancy}$ defects in reduced surfaces preferentially stabilizes 2L isomers.

It has been found that gold nanoparticles become globally positively charged when supported on stoichiometric TiO_2 and negatively charged when adsorbed on the reduced surface, although the present results indicate that this is not relevant for H_2 dissociation activity. Positively charged Au atoms are usually involved in Au−O−Ti bonds and are not able to coordinate and activate H_2; negatively charged gold atoms are usually highly coordinated inside or terrace-type atoms. Therefore, active Au atoms are neutral or with a net charge close to zero.

It has also been shown that the number of potentially active sites for H_2 dissociation, that are neutral corner or edge gold atoms in low coordination state and not directly bonded to the support, depends on the particle shape, which in turn is influenced by the type of support. The particles with the largest number of active sites are 2L isomers consisting of at least one bottom layer of gold atoms in contact with the support and therefore inactive, and one top layer separated from the support with low coordinated gold atoms on which H_2 is adsorbed and activated. The presence of $O_{vacancy}$ defects on the TiO_2 surface preferentially stabilizes these 2L particles, increasing the catalyst activity.

Acknowledgment. Financial support has been provided by the Spanish Ministry of Education and Science (grants MAT 2006-14274-C02-01 and CTQ2005-08459-CO2-01) and, in part, by Generalitat de Catalunya (2005SGR-00697). The authors thankfully acknowledge the computer resources, technical expertise, and assistance provided by the Barcelona Supercomputing Center/Centro Nacional de Supercomputación.

Supporting Information Available: Tables of coordination numbers and geometrical arrangement of Au atoms in the isolated Au_{13} nanoparticles at their optimized geometry; number of Au atoms in I, T, E, and C geometrical arrangements; summary of Bader atomic charges for each one of the supported Au_{13} models in the regular and defective (001) surface of anatase; and POSCAR files. This material is available free of charge via the Internet at http://pubs.acs.org.

References and Notes

(1) Hammer, B.; Norskov, J. K. *Nature* **1995**, *376*, 238.
(2) Fu, Q.; Saltsburg, H.; Flytzani-Stephanopoulos, M. *Science* **2003**, *301*, 935.
(3) (a) Haruta, M.; Kobayashi, T.; Sano, H.; Yamada, N. *Chem. Lett.,* **1987**, 405. (b) Haruta, M. *Catal. Today* **1997**, *36*, 153.
(4) (a) Valden, M.; Lai, X.; Goodman, D. M. *Science* **1998**, *281*, 1647. (b) Chen, M. S.; Goodman, D. W. *Science* **2004**, *306*, 252. (c) Meier, D. C.; Goodman, D. W. *J. Am. Chem. Soc.* **2004**, *126*, 1892.
(5) (a) Hutchings, G. J. *Gold Bull.* **2004**, *37*, 3. (b) Hutchings, G. J. *Catal. Today* **2005**, *100*, 55.
(6) (a) Carretin, S.; Concepción, P.; Corma, A.; Nieto, J. M. L.; Puntes, V. F. *Angew. Chem., Int. Ed.* **2004**, *43*, 2538. (b) Guzman, J.; Carrettin, S.; Corma, A. *J. Am. Chem. Soc.* **2005**, *127*, 3286.
(7) Porta, F.; Prati, L.; Rossi, M.; Scari, G. *J. Catal.* **2002**, *211*, 464l.
(8) Abad, A.; Concepción, P.; Corma, A.; García, H. *Angew. Chem., Int. Ed.* **2005**, *44*, 4066.
(9) Nijhuis, T. A.; Weckhuysen, B. M. *Catal. Today* **2006**, *117*, 84.
(10) (a) Hayashi, T.; Tanaka, K.; Haruta, M. *J. Catal.* **1998**, *178*, 566. (b) Chowdhury, B.; Bravo-Suarez, J. J.; Mimura, N.; Lu, J.; Bando, K. K.; Tsubota, S.; Haruta, M. *J. Phys. Chem. B* **2006**, *110*, 22995.
(11) (a) Carrettin, S.; Guzman, J.; Corma, A. *Angew. Chem., Int. Ed.* **2005**, *44*, 2242. (b) González-Arellano, C.; Abad, A.; Corma, A.; García, H.; Iglesias, M.; Sánchez, F. *Angew. Chem., Int. Ed.* **2007**, *46*, 1536.
(12) Bond, G. C.; Thompson, D. T. *Catal. Rev. Sci. Eng.* **1999**, *41*, 319.
(13) (a) Jia, J.; Haraki, K.; Kondo, J. N.; Domen, K.; Tamaru, K. *J. Phys. Chem. B* **2000**, *104*, 11153. (b) Choudhary, T. V.; Sivadinarayana, C.; Datye, A. K.; Kumar, D.; Goodman, D. W. *Catal. Lett.* **2003**, *86*, 1.
(14) (a) Bailie, J. E.; Hutchings, G. J. *Chem. Commun.* **1999**, 2151. (b) Bailie, J. E.; Abdullah, H. A.; Anderson, J. A.; Rochester, C. H.; Richardson, N. V.; Hodge, N.; Zhang, J. G.; Burrows, A.; Kiely, Ch. J.; Hutchings, G. J. *Phys. Chem. Chem. Phys.* **2001**, *3*, 4113.
(15) (a) Milone, C.; Tropeano, M. L.; Guline, G.; Neri, G.; Ingoglia, R.; Galvano, S. *Chem. Commun.* **2002**, 868. (b) Zanella, R.; Louis, C.; Giorgio, S.; Touroude, R. *J. Catal.* **2004**, *223*, 328.
(16) (a) Corma, A.; Serna, P. *Science* **2006**, *313*, 332. (b) Boronat, M.; Concepción, P.; Corma, A.; González, S.; Illas, F.; Serna, P. *J. Am. Chem. Soc.* **2007**, *129*, 16230.
(17) Claus, P. *Appl. Catal. A: General* **2005**, *291*, 222.
(18) Weiher, N.; Beesley, A. M.; Tsapatsaris, N.; Delannoy, L.; Louis, C.; van Bokhoven, J. A.; Schroeder, S. L. M. *J. Am. Chem. Soc.* **2007**, *129*, 2240.
(19) Schubert, M. M.; Hackenberg, S.; van Veen, A. C.; Muhler, M.; Plzak, V.; Behm, R. J. *J. Catal.* **2001**, *197*, 113.
(20) Hakkinen, H.; Abbet, S.; Sanchez, A.; Heiz, U.; Landman, U. *Angew. Chem., Int. Ed.* **2003**, *42*, 1297.
(21) Molina, L. M.; Hammer, B. *Appl. Catal. A: General* **2005**, *291*, 21, and references cited therein. .
(22) (a) López, N.; Janssens, T. V. J.; Clausen, B. S.; Xu, Y.; Mavrikakis, M.; Bligaard, T.; Norskov, J. K. *J. Catal.* **2004**, *223*, 232. (b) Remediakis, I. N.; Lopez, N.; Norskov, J. K. *Angew. Chem., Int. Ed.* **2005**, *44*, 1824.
(23) Hernández, N. C.; Sanz, J. F.; Rodriguez, J. A. *J. Am. Chem. Soc.* **2006**, *128*, 15600.
(24) Lemire, C.; Meyer, R.; Shaikhutdinov, S.; Freund, H. J. *Angew. Chem., Int. Ed.* **2004**, *43*, 118.
(25) Mavrikakis, M.; Stoltze, P.; Noskov, J. K. *Catal. Lett.* **2000**, *64*, 101.
(26) Turner, M.; Golovko, V. B.; Vaughan, O. P. H.; Abdulkin, P.; Berenguer-Murcia, A.; Tikhov, M. S.; Johnson, B. F. G.; Lambert, R. M. *Nature* **2008**, *454*, 981.
(27) Molina, L. M.; Hammer, B. *Phys. Rev. Lett.* **2003**, *90*, 206102.
(28) Liu, Z. P.; Gong, X. Q.; Kohanoff, J.; Sanchez, C.; Hu, P. *Phys. Rev. Lett.* **2003**, *91*, 266102.
(29) Liu, H.; Kozlov, A. I.; Kozlova, A. P.; Shido, T.; Asakura, K.; Iwasawa, Y. *J. Catal.* **1999**, *185*, 252.
(30) Wang, X. H.; Li, J. G.; Kamiyama, H.; Katada, M.; Ohashi, N.; Moriyoshi, Y.; Ishigaki, T. *J. Am. Chem. Soc.* **2005**, *127*, 10982.
(31) (a) Guzman, J.; Carrettin, S.; Fierro-González, J. C.; Gates, B. C.; Corma, A. *Angew. Chem., Int. Ed.* **2005**, *44*, 4778. (b) Carrettin, S.; Hao, Y.; Aguilar-Guerrero, V.; Gates, B. C.; Trasobares, S.; Calvino, J. J.; Corma, A. *Chem. Eur. J.* **2007**, *13*, 7771.
(32) Wahlström, E.; Lopez, N.; Schaub, R.; Thostrup, P.; Ronnau, A.; Africh, C.; Laegsgaard, E.; Norskov, J. K.; Besenbacher, F. *Phys. Rev. Lett.* **2003**, *90*, 026101.
(33) (a) Bus, E.; Miller, J. T.; van Bokhoven, J. A. *J. Phys. Chem. B* **2005**, *109*, 14581. (b) Mohr, C.; Hofmeister, H.; Radnik, J.; Claus, P. *J. Am. Chem. Soc.* **2003**, *125*, 1905.
(34) Mohr, C.; Hofmeister, H.; Claus, P. *J. Catal.* **2003**, *213*, 86.
(35) (a) Andrews, L.; Wang, X. F. *J. Am. Chem. Soc.* **2003**, *125*, 11751. (b) Andrews, L.; Wang, X. F.; Manceron, L.; Balasubramanian, K. *J. Phys. Chem. A* **2004**, *108*, 2936. (c) Andrews, L. *Chem. Soc. Rev.* **2004**, *33*, 123.

(36) Varganov, S. A.; Olson, R. M.; Gordon, M. S.; Mills, G.; Metiu, H. *J. Chem. Phys.* **2004**, *120*, 5169.
(37) Ghebriel, H. W.; Kshirsagar, A. *J. Chem. Phys.* **2007**, *126*, 244705.
(38) Okumura, M.; Kitagawa, Y.; Haruta, M.; Yamaguchi, Y. *Appl. Catal., A* **2005**, *291*, 37.
(39) Barrio, L.; Liu, P.; Rodriguez, J. A.; Campos-Martín, J. M.; Fierro, J. L. G. *J. Chem. Phys.* **2006**, *125*, 164715.
(40) Barton, D. G.; Podkolzin, S. G. *J. Phys. Chem. B* **2005**, *109*, 2262.
(41) (a) Wells, D. H.; Delgass, W. N.; Thomson, K. T. *J. Catal.* **2004**, *225*, 69. (b) Joshi, A. M.; Delgass, W. N.; Thomson, K. T. *Top. Catal.* **2007**, *44*, 27.
(42) Corma, A.; Boronat, M.; González, S.; Illas, F. *Chem. Commun.* **2007**, 3371.
(43) Gong, X. Q.; Selloni, A. *J. Phys. Chem. B* **2005**, *109*, 19560.
(44) Yang, H. G.; Sun, C. H.; Qiao, S. Z.; Zou, J.; Liu, G.; Smith, S. C.; Cheng, H. M.; Lu, G. Q. *Nature* **2008**, *453*, 638.
(45) (a) Kresse, G.; Furthmüller, J. *Phys. Rev. B* **1996**, *54*, 11169. (b) Kresse, G.; Hafner, J. *Phys. Rev. B* **1993**, *47*, 558.
(46) (a) Perdew, J. P.; Chevary, J. A.; Vosko, S. H.; Jackson, K. A.; Pederson, M. R.; Singh, D. J.; Fiolhais, C. *Phys. Rev. B* **1992**, *46*, 6671. (b) Perdew, J. P.; Wang, Y. *Phys. Rev. B* **1992**, *45*, 13244.
(47) Blöchl, P. E. *Phys. Rev. B* **1994**, *50*, 17953.
(48) Bader, R. F. W. *Atoms in Molecules: A Quantum Theory*; Oxford Science: Oxford, UK, 1990.

JP808271Y